Molecular versus Electromagnetic Wave Propagation Loss in Macro-Scale Environments

Weisi Guo[1], Christos Mias[1], Nariman Farsad[2], Jiang-Lun Wu[4]

***Abstract*—Molecular communications (MC) has been studied as a bio-inspired information carrier for micro-scale and nano-scale environments. On the macro-scale, it can also be considered as an alternative to electromagnetic (EM) wave based systems, especially in environments where there is significant attenuation to EM wave power. This paper goes beyond the unbounded free space propagation to examine three macro-scale environments: the pipe, the knife edge, and the mesh channel. Approximate analytical expressions shown in this paper demonstrate that MC has an advantage over EM wave communications when: (i) the EM frequency is below the cut-off frequency for the pipe channel, (ii) the EM wavelength is considerably larger than the mesh period, and (iii) when the receiver is in the high diffraction loss region of an obstacle.**

I. Introduction

A. Background

Molecular communication is a system that utilizes chemical particles as a carrier for information. The information can be repetitive signalling from a limited alphabet, which is common in biological systems; or generic information from a rich alphabet, which is more common in human interaction. Historically, molecular-based signalling between animals has been observed since the ancient times, and more explicit arguments relating signalling success and natural selection was articulated by Darwin in 1871 [1]. It is only in the last decade or so that molecular communication from a telecommunications and information theory perspective has been explored [2]. Primarily, this has been due to the rise in demand from nano-scale engineering (e.g., communication between swarms of nano-robots for targeted drug delivery [3]) and also the demand for industrial sensing in adverse environments [4]. In both of these cases, the local environment can be adverse to the efficient propagation of electromagnetic (EM) wave signals.

Over the past decade, a growing body of significant molecular communication research has been devoted to a wide range of: channel modeling [5] and telecommunication system design [6], [7], information theory [8], [9], sensor and circuit design [10]. A number of metrics are needed to gauge the performance of an entire new species of communications. To list some: coverage area, reliability, capacity bound, and bandwidth availability. However, MC is a relatively new area, many fundamental issues are unresolved or at least not agreed upon in the research community. In this paper, we can only focus on one fundamental aspect which is propagation comparison in different scenarios. We hope this paper on propagation loss comparison can provide the foundation for others to build towards higher level metrics such as capacity and coverage.

Despite these recent tentative first steps to building a molecular communication system, it remains unclear what the precise advantages of conveying information by molecules are. If we look towards nature, as far as we know, no known animal or organism uses EM-wave based communications, and yet many animals such as the platypus and electric eel can generate strong electric fields to communicate and navigate [11]. On the other hand, a variety of biological creatures use chemical messaging, both at the macro-scale across great distances (e.g., Moths can communicate several km using pheromone signalling over the air [1]) and at the nano-scale between cells. This tempts us to ask: *what is the advantage of molecular communications over EM-waves communications?*

One fundamental difference we do know is the difference between random walk propagation and wave propagation. In this paper, we suspect that random walk propagation may yield advantages in certain propagation environments. In fact, earlier work has already shown experimentally that EM-waves can propagate inefficiently in tunnel / maze environments, whereas molecular communications retain the shape of the channel response irrespective of the maze environment and almost always deliver the data successfully, albeit a long delay [12]. The potential applications [2], include the communication between robots in underground tunnels or the extraction of embedded sensor data from cavities or machinery. This has led us to give a more comprehensive theoretical analysis in comparing the difference between molecular and EM-wave propagation for the purpose of understanding their relative propagation advantages.

B. Contribution & Organisation

This paper aims to emphasise the potential of molecular propagation in the field of macro-scale wireless communications. Simple approximate closed form expressions for EM wave propagation are used to show the demarkation between efficient EM wave transmission and efficient molecule transmission. While, recently, a comprehensive research survey [13] has qualitatively described molecular and EM communication in nano-networks, to the best of our knowledge, there has been no quantitative comparison between their loss in different macro-scale channels other than free-space. Thus, the contribution in this paper is to set out the demarcation between efficient EM wave propagation and molecular diffusion, in terms

[1]School of Engineering, University of Warwick, UK. [2]Deptartment of Electrical Engineering and Computer Science, York University, Canada. [4]Department of mathematics, Swansea University, UK. Corresponding author e-mail: weisi.guo@warwick.ac.uk This work has been funded by the Royal Society Grant IE130762.

of geometric parameters, EM wave frequency and diffusion parameters. The rationale for considering the pipe, knife-edge, aperture, and mesh geometric scenarios are because approximations of the channels can be found in the natural (e.g. caves) and built (cages, apertures in metallic structures) environments [14]. The comparison of EM and molecular propagation in liquid channels where electromagnetic waves normally suffer significant absorption will be considered in future. We believe this is a step towards the future development of tandem EM wave and molecular systems and the future planning of the deployment of molecular communication systems.

In terms of methodology and difficulty, accurate EM and MC pathloss equations are difficult to obtain. Experimentally, the authors have compared EM and MC pathloss in pipe network environments [12]. As for theoretical work propagation in non-free-space environments (i.e., with obstacles), there is limited work. As far as we are aware, the first monograph where first-passage processes are derived is found in [15]. The challenge of reflections and absorptions at the boundary conditions makes the propagation equations difficult to derive. To the best of our knowledge, for molecular diffusion, the most advanced progress in deterministic geometric obstacles is made in deriving only the first passage time distribution of random walk over a planar wedge [16], [17].

The paper is organised as follows. In Section II, approximate analytical expressions for the free space propagation of EM waves and diffusion of molecules are revisited for completeness. Sections III to V consider propagation channels: (i) the pipe, (ii) the knife-edge, and (iii) the mesh channel.

II. Review of Free-Space Environment

We first review the unbounded free-space environment. This will serve two purposes: to introduce fundamental free-space (FS) equations for later use, and to benchmark performance comparisons between EM and MC. We consider EM waves in the radio- and micro-wave frequency range [1]. We define gain as the ratio between the received and the transmitted power for EM signals or received and the transmitted energy for molecular signals. EM wave propagation is considered in the frequency-domain, for which simple approximate formulae exist describing signal power attenuation or gain for the three channels under considered.

A. Power Attenuation Definition

The power attenuation or gain (expressed in dB) is traditionally employed in EM communication and serves as a metric of the successful operation of a communication system. The receiver sensitivity determines the acceptable level of power attenuation. We employed the energy metric in MC which is associated with time-domain pulse transmission [19] and for which simple approximate formulae are derived in this work. These formulae are derived based on time integration. The longer the integration time the larger the received energy. Although the use of different metrics in different domains prevents direct comparison between EM and molecular signal transmission, the use of simple power/energy expressions, such as the one used in this work, provides insight into signal level attenuation and will allow one to approximately determine the presence or not of a communication link once receiver sensitivity values are known. Hence, the emphasis of this paper is on presenting plots of EM power attenuation or MC energy level with respect to transmitter/receiver distance and across obstacles.

1) EM Pathloss: Assuming the EM waves radiate from a point source, the power gain (Λ_P) at distance d is:

$$\Lambda_{\text{FS,EM},P}(d,f) = \left(\frac{4\pi df}{c}\right)^{-2}, \tag{1}$$

where f is the frequency and c is the speed of light in a vacuum. The time of arrival of the wave is $\tau = d/c$.

2) MC Pathloss: For molecules that diffuse from a point source in free-space, a more appropriate measure of loss can be derived first from the hitting probability density function (pdf) [20], [21]:

$$p_{\text{FS,MC}}(d,D,t,\rho) = \frac{1}{(4\pi Dt)^{\rho}} \exp\left(-\frac{d^2}{4Dt}\right), \tag{2}$$

where D is the diffusivity (governs the rate of diffusion) and the exponent ρ varies with the number of dimensions, such that: 1-dimensional space ($\rho = 1/2$), 2-dimensional space ($\rho = 1$), and 3-dimensional space ($\rho = 3/2$). The aforementioned equation can be derived from first principle when considering the position distribution of a particle restricted to random motion of a unit steps [20]. As shown recently in [19], the molecular energy gain (Λ_E) in 3-dimensional space can be found by integrating Eq.(2) over the reception time T:

$$\Lambda_{\text{FS,MC},E}(d,D) = \lim_{T\to+\infty} \int_0^T p_{\text{FS,MC}}\,\mathrm{d}t = (4\pi Dd)^{-1}. \tag{3}$$

The maximum hitting probability (pulse amplitude) is detected at $\tau = d^2/6D$ and the corresponding value is $[3/(2\pi e)]^{3/2} d^{-3}$.

It is worth noting that further work have considered variations of Eq.(2) by including a receiver that absorbs molecules [5], [22] and also for disruptive laminar flow against the direction of communications [23]. More complex simulation work that involves the interaction of attraction and repulsion forces is presented recently in [24].

B. Comparison

Comparing EM wave and MC propagation, one should note that: (i) the gain of EM wave power is inverse-square proportional to the frequency f and distance d. The gain of the molecular energy is inversely proportional to the the diffusivity D and distance d; and (ii) the time of arrival of EM waves is not dependent on the carrier frequency f, and increases linearly with distance d. The time of arrival of molecules is dependent on the diffusivity D and increases quadratically with distance d. For free-space propagation, from a communications perspective, one can surmise the following.

[1]The EM equations in this paper can be applied at high frequencies, for example, the knife-edge model was experimentally shown to be applicable at 300GHz (millimetres) [18]. The MC equations are applicable across all the distances from nano- to kilometres

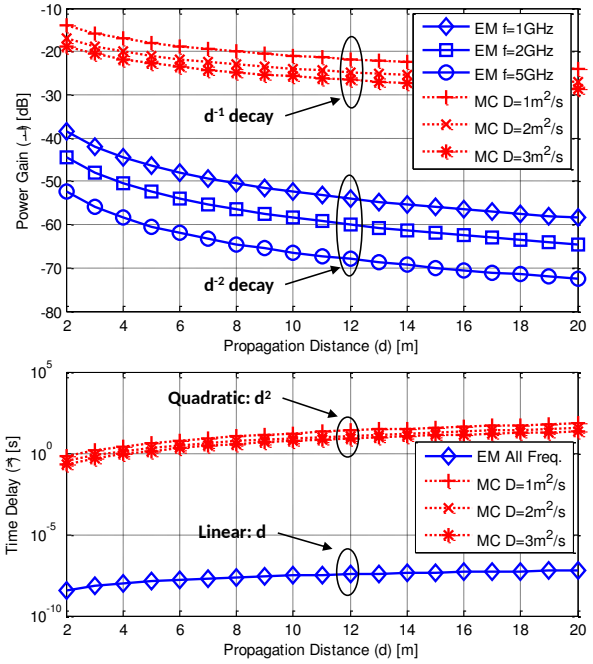

Fig. 1. Top: Free-space gain of EM signal power and MC signal energy versus different distances d for different EM frequencies f and different molecular diffusivity D. Bottom: Time delay τ versus distance d for different EM frequencies f and different molecular diffusivity D. The results are analytical.

As shown in Fig. 1, EM wave signals offer small delay ($\tau \sim 1$ns) communications with a power gain that is inverse-square proportional with the frequency and distance $\propto (fd)^{-2}$. Molecular signals offer long delay ($\tau \sim 1$s) communications with an energy gain that is inverse proportional to the the diffusivity [2] and distance $\propto (Dd)^{-1}$.

These initial results have shown that in free-space, molecular communication (MC) energy attenuates at a lower rate than EM wave signals. However, moving away from the idealized free-space models, the explicit boundaries that divide reliable MC from reliable EM wave based communications remains unclear, especially in environments that can significantly attenuate EM waves. This paper will set out the demarcation in terms of the propagation environment, as well as key wave and diffusion parameters.

III. Metallic Pipe Channel

Metallic pipes can be found in a variety of civil and industrial environments and have varying applications such as water supply and ventilation. It will be of interest to consider the molecular and EM wave propagation characteristics when the need arises to communicate information within a long metallic pipe [4], [14]. We only consider a single pipe, as opposed to a branching network, of rectangular cross-section. As an example, let us consider a pipe with a rectangular cross-section of width a, height b, and length d, as shown in Fig. 2. The material inside the pipe is assumed to be free space.

[2]The diffusivity values are chosen in this paper to allow for visual comparison on how gain varies with per unit distance for EM and MC systems.

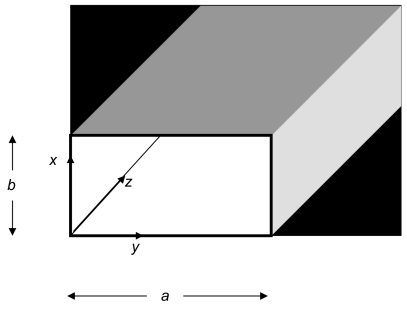

Fig. 2. Illustration of pipe's rectangular cross section with width a, height b, and a variable length.

A. EM wave Propagation

1) Loss-less Walls: From the EM wave propagation point of view, the dimensions of the cross-section of the pipe dictate the propagation of its transverse electric (TE_{mn}) and transverse magnetic (TM_{mn}) modes, i.e., the cut-off frequency f_{c} of each mode below which no EM wave power propagates in the waveguide. In our example, the mode with the lowest cutoff frequency is the TE_{10} mode and hence EM wave signals with frequencies less than the cut-off frequency of this mode, given by [25]:

$$f_{\text{c,Pipe}}(a) = \frac{1}{2a\sqrt{\mu_0 \epsilon_0}}, \tag{4}$$

cannot carry any power along the pipe. In Eq.(4), ϵ_0 and μ_0 are the permittivity and permeability constants of free-space. In contrast, signals of higher frequencies can carry power which, for wave-guides with perfectly electrically conducting walls, can be considered to propagate un-attenuated.

2) Lossy Walls: In real life however pipes are made of finite conductivity metals and hence the transmitted signal power is absorbed. The power gain is given by [25]:

$$\Lambda_{\text{Pipe,EM},P}(a,b,d,f) = \exp\left[-2d\sqrt{\frac{\pi f \epsilon_0}{\sigma b^2}} \frac{1+\frac{2b}{a}\left(\frac{f_{\text{c,Pipe}}}{f}\right)^2}{\sqrt{1-\left(\frac{f_{\text{c,Pipe}}}{f}\right)^2}}\right], \tag{5}$$

where σ is the conductivity.

In Fig. 3 the power loss of the EM wave signal is plotted against the propagation distance for two frequencies. The gain improves as the frequency of operation increases above the cut-off frequency $f_{\text{c,Pipe}}$. The conductivity of the copper pipe is $\sigma = 5.7 \times 10^7$ S/m. The dimensions of the pipe's rectangular cross-section are assumed to be $a = 5$cm and $b = 3$cm.

B. MC Propagation

For molecular propagation, the pipe environment can be modelled as semi-infinite 1-dimensional channel. Given that the pipe cross section is consistent and small compared to the length of the pipe channel, the effect of the boundary conditions have been shown experimentally to be negligible, and the gain only depends on the distance and the temperature

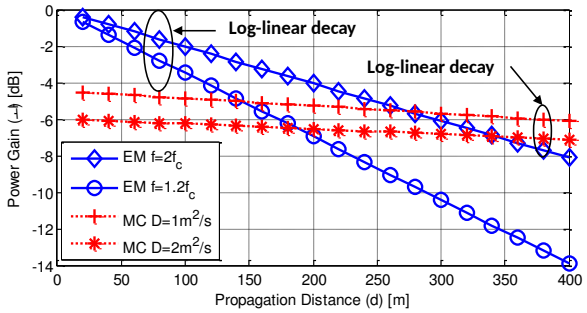

Fig. 3. Pipe channel gain of signal power and energy; as a function the pipe cross-section dimensions ($a = 5$cm, $b = 3$cm), distance d and: frequency f for EM waves, and diffusivity D for molecules. The results are analytical.

dependent diffusivity [12]. The energy gain can be found using a numerical integration method for single sided 1-dimensional diffusion over a reception period of T:

$$\Lambda_{\text{Pipe,MC},E}(d, D) = \lim_{T\to+\infty} 2\int_0^T p_{\text{FS,MC}}(d, D, t, \rho = 0.5)\,\mathrm{d}t \tag{6}$$

The gain for molecular diffusion in this case decays in a log-linear (exponential) relationship with distance $\propto \exp(-d)$ for a sufficiently large reception time [3]. The time τ to peak is given as $\tau = d^2/2D$.

In Fig. 3, we present the copper pipe channel gain as a function of the distance d and frequency f for EM waves, and diffusivity D for molecules. The results show that both the EM wave power and MC energy decay log-linearly (exponentially) with distance. In the lossy copper pipe scenario, the energy loss per unit length is lower for the MC than the power loss per unit length for EM waves for the particular set of parameters chosen.

IV. Knife Edge / Aperture Channels

The knife edge channel is used as a simple approximate model for calculating EM wave propagation over hills and buildings. Knife-edge type objects are often found at the macro-scale in urban and rural environments. As illustrated in Fig. 4, we consider a point source transmitter (Tx) and a point receiver (Rx) obstructed by a thin, *absorbing screen* having a height of H, and an aperture (slit) of width δ, which is larger than the EM wavelength.

A. EM wave Propagation

The following approximate diffraction coefcient formula for the aperture (diffraction by long slit), in terms of the cosine and sine Fresnel integrals, is readily obtained based on the knife edge derivation presented in [26]:

$$\mathcal{D} = \frac{\Phi(\upsilon_{H+\delta}) - \Phi(\upsilon_H)}{1-j}, \tag{7}$$

where $\Phi(\upsilon) = C(\upsilon) - jS(\upsilon)$, and where $C(\upsilon)$ and $jS(\upsilon)$ are cosine and sine Fresnel integrals and υ_H is the diffraction

[3]Strictly speaking, the reception time T cannot approach infinity as the integral does not converge.

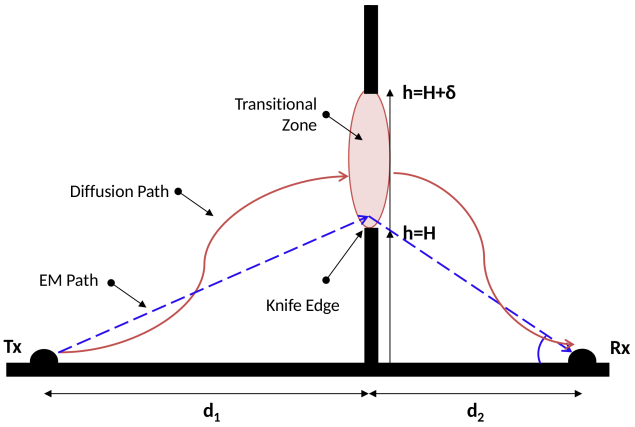

Fig. 4. Illustration of knife edge or aperture scenario with a transmitter (Tx) and receiver (Rx) on the same horizontal reference line, obstructed by a thin and non-penetrable and non-absorbing object with height H. A gap (transition zone) exists $H \le \delta < +\infty$.

parameter, such that for a height H:

$$\upsilon_H \approx H\sqrt{\frac{2(d_1+d_2)}{\lambda d_1 d_2}}. \tag{8}$$

The knife-edge diffraction coefficient is obtained in the limit of $\delta \to +\infty$ and since $\Phi(\infty) = \frac{1-j}{2}$, it follows that [27]:

$$\mathcal{D} = \frac{1}{2}[1 - (1+j)\Phi(\upsilon_H)], \tag{9}$$

which is valid provided the following conditions hold [27]: (i) $(d_1, d_2 \gg H)$; and (ii) $(d_1, d_2 \gg \lambda)$.

The power gain between a point source transmitter and a receiver is given by:

$$\Lambda_{\text{Knife,EM},P}(H, d, f) = \Lambda_{\text{FS,EM},P}|\mathcal{D}|^2, \tag{10}$$

where $\Lambda_{\text{FS,EM},P}$ is the 3-dimensional free-space gain that we defined in (1) and $|\mathcal{D}|^2$ is the knife-edge diffraction loss. In the simulations, the knife-edge diffraction loss is calculated using the Lee approximation [26].

B. MC Propagation

As considered in the EM case, we model an *absorbing screen* having a height of H, and an aperture (slit) of width δ, which is larger than the dimension of the molecules. There is not many existing literature tackling this problem. For molecular diffusion through the slit in the obstacle, we consider the random walk between two fixed points: one is on the left side of the obstacle with distance d_1 to the obstacle, and the other is on the right side of the obstacle with distance d_2 to the obstacle. We have then $p_{T_1}(d_1, h, D, t)$ the transitional pdf for the left random walk from the point $(-d_1, 0)$ to the point $(0, h)$, and like wise $p_{T_2}(d_2, h, D, t)$ the transitional pdf for the right random walk from the point $(0, h)$ to the point $(d_2, 0)$. The transitional pdfs are half-planar hitting pdfs:

$$p_{\text{T}}(d, h, D, t) = \frac{1}{2\pi Dt}\exp\left(-\frac{d^2+h^2}{4Dt}\right), \tag{11}$$

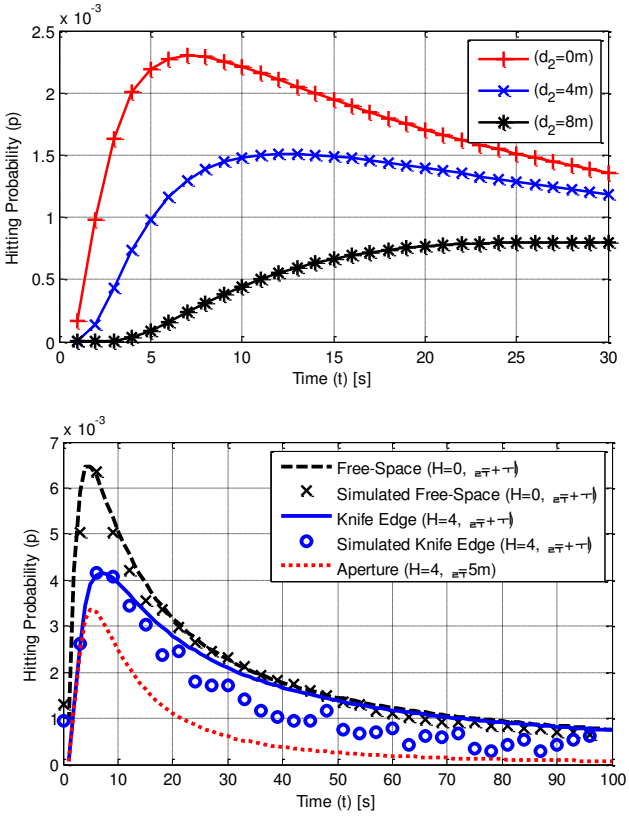

Fig. 5. Top: Hitting pdf as a function of different receiver distances d_2 with a fixed diffusivity D, obstacle height $H = 4$m and transmitter location $d_1 = 0$m. Bottom: Hitting pdf as a function of different aperture sizes δ and obstacle heights $H = 4$m, with a fixed diffusivity D, and transmitter and receiver locations $d_1 = d_2 = 3$m. The results are both analytical and from Monte-Carlo simulations.

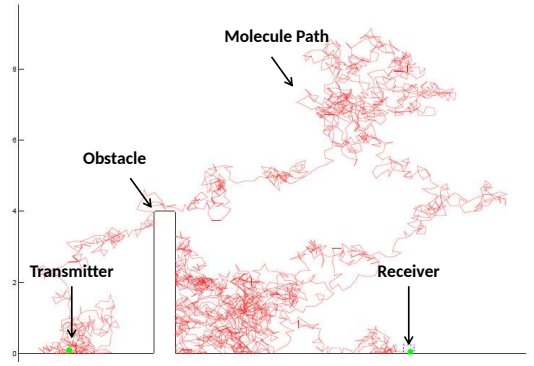

Fig. 6. A snap-shot of the Monte-Carlo simulation for a knife-edge channel.

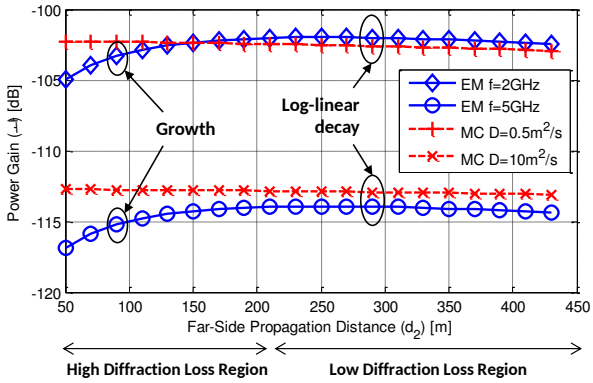

Fig. 7. Knife-edge channel gain of EM signal power and MC energy as a function of receiver distance d_2, for different EM frequencies f, and molecular diffusivity D. The results are analytical and the MC results are off-set to be on the same scale as EM results.

where $d = d_1$ for the transmitter side T_1 and $d = d_2$ for the receiver side T_2.

Interpreting the transitional pdfs as wave frequencies, the efficient frequency from source to destination is the convolution of the two involved frequencies p_{T_1} and p_{T_2}. That is the hitting pdf for the random traveling, which is described as a pinned Brownian motion with the two fixed points $(-d_1, 0)$ and $(d_2, 0)$. This is the convolution $p_{T_1} * p_{T_2}$ for the valid range $h \geq H$:

$$\begin{aligned} p_{\text{Knife,MC}}(d_1, d_2, t, H) &= \int_{h=H}^{+\infty} p_{\text{T1}} * p_{\text{T2}} \, \mathrm{d}h \\ &= \frac{\exp(-\frac{d_1^2+d_2^2}{4Dt})}{(4\pi Dt)^2} \int_{h=H}^{+\infty} \int_0^h \exp\left(-\frac{z^2+(h-z)^2}{4Dt}\right) \mathrm{d}z \, \mathrm{d}h \\ &= \frac{\exp(-\frac{d_1^2+d_2^2}{4Dt})}{4\pi Dt} \mathrm{erfc}\left(\frac{H}{\sqrt{8Dt}}\right)^2. \end{aligned} \tag{12}$$

For verification of the hitting pdf, we use a proprietary 2-D molecule Monte-Carlo simulator [28]. From Fig. 5, we can see that the peak responses largely agree, but the tail end of the MC knife-edge pdf is over optimistic in comparison with the Monte-Carlo simulation results. In both cases, the simulated results are reasonably accurate compared to the theoretical expressions, especially the peak arrival value and time. For the simulations, 25 million particles are assumed to be released and the hitting probability (not normalized) is recorded over a period of 100 seconds. A snap-shot of the Monte-Carlo simulation for a knife-edge channel is shown in Fig. 6.

If we examine the hitting pdf in Eq.(12), it essentially has two elements:

1) **the 2-dimensional Planar Hitting pdf** which inverse exponentially scales as a function of the shortest distance *through* the obstacle (d_1 and d_2);
2) **the Complementary Error Gain Function** which decays from 1 to 0 as a function of increasing obstacle size H.

A more general version of this problem is the hitting probability through an aperture, which can be found in the Appendix B in Eq.(18). The full proof of the double Gaussian integral can be found in Appendices A and B. The condition for when aperture is equivalent to knife edge is:

$$\mathrm{erf}\left(\frac{H+\delta}{\sqrt{8Dt}}\right)^2 \approx 1, \tag{13}$$

which occurs when either: (i) the obstacle is tall (e.g., a mountain), or (ii) the aperture is large.

We now consider two special cases of the aperture channel of Fig. 4:

1) Scenario A (Variable Receiver Distance): the transmitter

is fixed at $d_1 = 0$ and the receiver distance d_2 varies. The height of the obstacle $H = 4$m is fixed.

2) Scenario B (Variable Aperture): both the transmitter and the receiver are placed in fixed locations, and the aperture has a variable size such that $0 < \delta < +\infty$, where $\delta \to +\infty$ is the knife edge example.

In Fig. 5, the corresponding hitting pdfs for Scenarios A and B are shown. In Fig. 5(top), which is Scenario A, a fixed obstacle of height $H = 4$m and transmitter position of $d_1 = 0$m at the base of the obstacle was considered. The receiver was placed at variable distances ($d_2 = 0$ to 8m). The resulting hitting pdfs show that as the receiver moves further from the obstacle, a greater delay (τ) to peak is expected, as well as a smoother hitting pdf. Generally speaking, receivers not in high diffraction loss positions perform worse than those in high diffraction loss for MC, because the shortest path from transmitter to receiver is longer. In Fig. 5(bottom), which is Scenario B, an aperture is considered. The lower boundary of the aperture has height $H = 4$m and a aperture sizes of $\delta = 5$m and infinity are considered. The transmitter and receiver are both placed at a distance of 3m away from the obstacle. The resulting hitting pdfs show that as the aperture size increased, it gradually becomes the knife edge model. As mentioned previously, the simulation results from a Monte-Carlo simulator to validate the theoretical model.

We now compare MC energy with EM power gain. For the knife-edge example, the resulting received MC energy can be found as: $\Lambda_{\text{Knife,MC},E}(d_1, d_2, H) = \lim_{T\to+\infty} \int_0^T p_{\text{Knife,MC}}(d_1, d_2, t, H)\,\mathrm{d}t$. The gain for molecular diffusion in this case decays in a log-linear relationship with distance for a sufficiently large value of T. In Fig. 7, we present the knife edge channel gain as a function the receiver distance d_2 for different EM wave frequencies and molecular diffusivity D. The results show that the EM knife edge gain reduces as the distance d_2 increases; and for sufficiently large distance d_2, the EM loss per unit length is log-linear. For MC, the gain always reduces log-linearly with distance.

V. Mesh Channel

Wire meshes find many applications, most of which are not designed with EM wave propagation in mind, such as fences and cages. As an example, we consider a (bonded) orthogonal square unit cell mesh, shown in Fig. 8, consisting of thin wires of radius r and period R.

A. EM Wave Propagation

Meshes can attenuate the power of an incident EM signal through absorption, reflection and cross-polarisation. For a sufficiently small period compared with the wavelength, one can obtain simple expressions for the plane wave transmission coefficient through the mesh for both parallel and perpendicular polarisation [29]. The transmission coefficient depends on the angle of incidence, the incident wave polarisation, the geometric parameters of the mesh, and the frequency. For this electrically small period case, cross-polarisation can be neglected. Furthermore, the transmission coefficient expressions for the two polarisations merge into a single one if one assumes normal incidence, as it is assumed here for simplicity. Also for simplicity, it it assumed that mesh absorption can be neglected. Hence, for point source transmitter and receiver, the gain may be approximated as (this problem may be considered as a one wall Keenan-Motley model [30]):

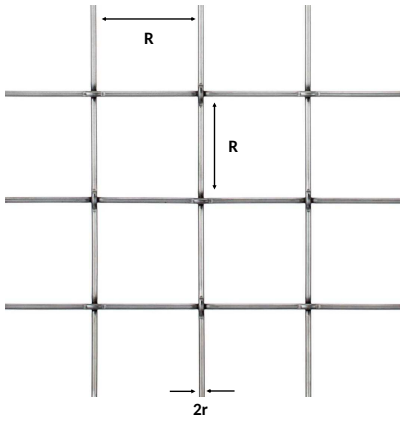

Fig. 8. Illustration of mesh with cylindrical wires of radius r and separation period R.

$$\Lambda_{\text{Mesh,EM},P}(r, R, f) = \Lambda_{\text{FS,EM},P}|1 - \frac{\eta}{\eta - 2Z_g}|^2, \qquad (14)$$

where $\eta = \sqrt{\mu_0/\epsilon_0}$, $Z_g = -jf\mu_0 R \ln(1 - \exp(-2\pi r/R))$, and $\Lambda_{\text{FS,EM},P}(\nu = 1)$ is the free-space gain without the mesh.

B. MC Propagation

For molecular propagation, the mesh environment can be modeled as 3-dimensional propagation model. The effect of the mesh wires is assumed to be negligible for a sufficiently large R/r ratio. The energy gain is the same as that of free-space:

$$\Lambda_{\text{Mesh,MC},E}(d, D) \approx \Lambda_{\text{FS,MC},E}(d, D, \rho = 3/2) = \frac{1}{4\pi D t}. \qquad (15)$$

The gain for molecular diffusion in this case decays in an inverse relationship with distance ($\propto d^{-1}$) for a sufficiently large value of $T \to \infty$.

In Fig. 9 (top), we present the mesh gain as a function of the mesh period R for different frequencies. From the results, we can see that as the mesh period increases with respect to the EM wavelength, the gain increases. For a mesh period of $R = 0.03$m and wire radius $r = 0.25$mm, Fig. 9 (top) shows that the gain difference between the 0.5GHz and 1GHz signals is 5dB. In Fig. 9 (bottom), we place the mesh 10m away from the point transmitter source. Then we also assume a point receiver source. We observe a similar trend to the EM free-space results shown previously in Fig. 1, except that the signal suffers an additional loss at the mesh's location. For comparison, we also plotted the 3-dimensional FS MC results. This demonstrates the advantage of MC, suffering negligible loss due to the mesh.

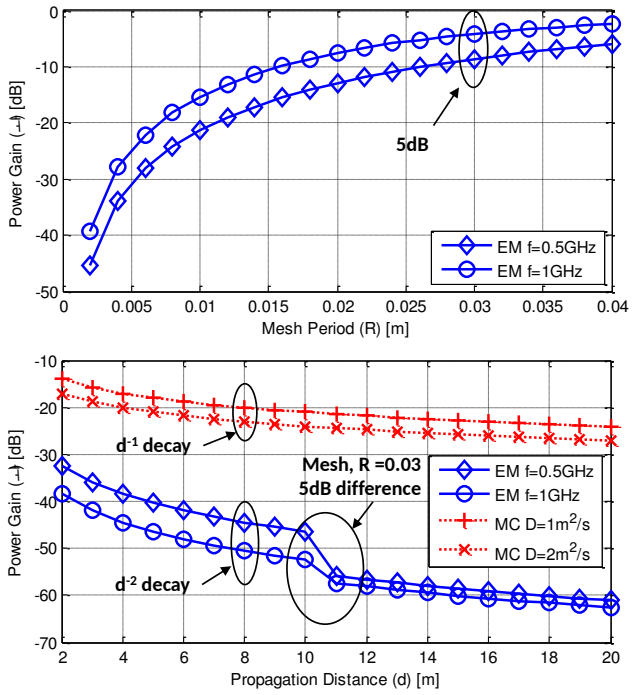

Fig. 9. Top: Mesh gain of EM signal power as a function of the mesh duration R for different EM frequencies f. Bottom: Mesh gain of EM signal power and MC energy as a function of the propagation distance (d) for different EM frequencies f and MC diffusivity D. A mesh with period $R = 0.03$m is positioned at a distance of 10m from the source.

VI. Conclusions and Future Work

Comparison between the molecular and electromagnetic wave propagation loss in macro-scale channels was extended, for the first time, beyond free-space to consider a pipe channel, a knife edge channel and a mesh channel. In doing the comparison, simple approximate analytical formulations were used that provide insight into the behaviour of the signals. The aim was to identify scenarios and parameters for which the molecular signal energy propagation loss was lower than the power loss of the propagated electromagnetic signals.

For the copper pipe, the channel attenuation as a function of the pipe length, electromagnetic wave frequency and molecular diffusivity was considered. It was shown that for a lossy pipe both the electromagnetic power and the molecular communication energy decay log-linearly with distance. However, the attenuation per unit length was lower for the molecular than for the electromagnetic wave propagation. For the knife-edge channel, the attenuation as a function of the receiver distance from the obstacle was presented for different electromagnetic wave frequency and the molecular diffusivity. The results showed that electromagnetic wave attenuation increased as the receiver distance from the obstacle was decreased. However, no such behaviour was observed for the molecular signal whose attenuation was always increasing log-linearly with distance. It is also worth noting, that for the molecular propagation our novel knife-edge hitting probability results were found to agree well with those of simulations. Finally, for the thin wire mesh channel, it was shown that the attenuation of the electromagnetic signal increases, for a given wavelength, as the period of the mesh decreases. For the molecular signal however one anticipates that the effect of the mesh will not be as significant.

Based on the results of this work, one expects that molecular communication may have an advantage over electromagnetic communication in more complex environments where multiple obstacles are present. It is also unclear how ultra-high frequency EM communications will compare to MC in liquid environments of different viscosities. How the discoveries made in this paper along with the aforementioned factors and different noise models ultimately contribute to the information theoretic capacity is not known. These unexplored areas will be the subject of future work.

Appendix

A. Convolution of Two Transition Probability Densities

From Eq.(12), we have for an aperture channel (Ap.):

$$p_{\text{Ap.,MC}}(d_1, d_2, t, H) = \int_{h=H}^{H+\delta} p_{\text{T1}} * p_{\text{T2}}\, \mathrm{d}h. \tag{16}$$

The convolution with respect to h is:

$$\begin{aligned} p_{\text{T1}} * p_{\text{T2}} &= \int_0^h p_{\text{T1}}(z) p_{\text{T1}}(h-z)\, \mathrm{d}z \\ &= \frac{\exp\left(-\frac{d_1^2+d_2^2}{4Dt}\right)}{(2\pi Dt)^2} \int_0^h \exp\left(-\frac{z^2+(h-z)^2}{4Dt}\right) \mathrm{d}z \\ &= \frac{\sqrt{2\pi Dt}\exp\left(-\frac{d_1^2+d_2^2}{4Dt} - \frac{h^2}{8Dt}\right)}{(2\pi Dt)^2} \mathrm{erf}\left(\frac{h}{\sqrt{8Dt}}\right) \end{aligned} \tag{17}$$

B. Hitting PDFs for Aperture and Knife Edge Scenario

Combining Eq.(12) with Eq.(17), we can consider a transition zone of size H to $H+\delta$:

$$\begin{aligned} p_{\text{Ap.,MC}} &= \int_H^{H+\delta} \frac{\exp(-\frac{d_1^2+d_2^2}{4Dt} - \frac{h^2}{8Dt})}{(2\pi Dt)^{3/2}} \mathrm{erf}\left(\frac{h}{\sqrt{8Dt}}\right) \mathrm{d}h \\ &= \frac{\exp(-\frac{d_1^2+d_2^2}{4Dt})}{4\pi Dt} \left[\mathrm{erf}\left(\frac{H+\delta}{\sqrt{8Dt}}\right)^2 - \mathrm{erf}\left(\frac{H}{\sqrt{8Dt}}\right)^2\right]. \end{aligned} \tag{18}$$

For $\delta \to +\infty$, the knife edge hitting pdf is:

$$p_{\text{Knife,MC}} = \frac{\exp(-\frac{d_1^2+d_2^2}{4Dt})}{4\pi Dt} \mathrm{erfc}\left(\frac{H}{\sqrt{8Dt}}\right)^2. \tag{19}$$

Weisi Guo is an Assistant Professor at the University of Warwick. He received his M.Eng., M.A. and Ph.D. degrees from the University of Cambridge. He has published over 50 IEEE papers in recent years and won several academic awards, including being a finalist of the 2014 Bell Labs Prize. His research interests

are in the areas of 4G/5G cellular networks, smart cities, and molecular communications.

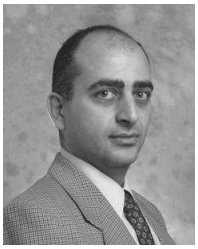

Christos Mias is an Associate Professor at the University of Warwick. He received his B.Eng. from the University of Bath and Ph.D. from the University of Cambridge. He served as the UK URSI Commission B (Fields and Waves) representative from 2009 to 2014, and he is interested in frequency selective surfaces, antennas, and radio-wave propagation.

Nariman Farsad is currently a final year Ph.D. student at York University. He was awarded 2nd Prize in the IEEE Communications Society's Student Project Award (2014). He is interested in bio-inspired communication systems and swarm intelligence, communication engineering aspects of neuroscience and biological systems, and biological computers.

Jiang-Lun Wu is a Professor at the University of Swansea. He graduated from Northwest University in Xian and received his Ph.D. in 1991 from the Chinese Academy of Sciences, Beijing, where he was appointed as associate professor in 1993. He was awarded A v Humboldt Research Fellow at Ruhr-University Bochum, Germany and then DFG research fellow. He is interested in partial differential equations, probability theory, functional analysis, financial mathematics and mathematical physics.

REFERENCES

[1] T. D. Wyatt, "Fifty years of pheromones," *Nature*, vol. 457, no. 7227, pp. 262–263, Jan. 2009.

[2] T. Nakano, A. Eckford, and T. Haraguchi, *Molecular Communication*. Cambridge University Press, 2013.

[3] S. Chandrasekaran and D. Hougen, "Swarm intelligence for cooperation of bio-nano robots using quorum sensing," in *IEEE Bio Micro and Nanosystems Conference*, Jan. 2006, p. 141.

[4] F. Stajano, N. Hoult, I. Wassell, P. Bennett, C. Middleton, and K. Soga, "Smart bridges, smart tunnels: Transforming wireless sensor networks from research prototypes into robust engineering infrastructure," *Ad Hoc Networks*, vol. 8, no. 8, pp. 872–888, Nov. 2010.

[5] B. Yilmaz, A. Heren, T. Tugcu, and C. Chae, "Three-dimensional channel characteristics for molecular communications with an absorbing receiver," *IEEE Commuminications Letters*, vol. 18, 2014.

[6] I. F. Akyildiz, F. Brunetti, and C. Blazquez, "Nanonetworks: a new communication paradigm," *Elsevier Computer Networks*, vol. 52, pp. 2260–2279, Aug. 2008.

[7] L. Felicetti, M. Femminella, G. Reali, T. Nakano, and A. V. Vasilakos, "TCP-like molecular communications," *IEEE Journal on Selected Areas in Communications (JSAC)*, vol. 32, no. 12, pp. 2354–2367, Dec. 2014.

[8] B. Atakan and O. Akan, "An information theoretical approach for molecular communication," in *IEEE Bionetics Conference*, Dec. 2007.

[9] K. Srinivas, A. Eckford, and R. Adve, "Molecular Communication in Fluid Media: The Additive Inverse Gaussian Noise Channel," in *IEEE Transactions on Information Theory*, vol. 8, Jul. 2012, pp. 4678–4692.

[10] M. Pierobon and I. F. Akyildiz, "A physical end-to-end model for molecular communication in nanonetworks," *IEEE Journal on Selected Areas in Communications*, vol. 28, no. 4, pp. 602–611, 2010.

[11] T. Wyatt, *Pheromones and Animal Behaviour: Communication by Smell and Taste*. Cambridge University Press, 2003.

[12] S. Qiu, W. Guo, S. Wang, N. Farsad, and A. Eckford, "A molecular communication link for monitoring in confined environments," in *IEEE International Conference on Communications*, 2014, pp. 718–723.

[13] N. Rikhtegar and M. Keshtgary, "A brief survey on molecular and electromagnetic communications in nano-networks," *International Journal of Computer Applications*, vol. 79, pp. 16–28, Oct. 2013.

[14] S.-U. Yoon, L. Cheng, E. Ghazanfari, S. Pamukcu, and M. T. Suleiman, "A radio propagation model for wireless underground sensor networks," in *IEEE Global Telecommunications Conference*, Dec. 2011.

[15] S. Redner, *A guide to first-passage processes*. Cambridge University Press, 2001.

[16] D. Dy and J. Esguerra, "First-passage-time distribution for diffusion through a planar wedge," *Physics Review E: Statistical, Nonlinear, and Soft Matter Physics*, vol. 78, no. 6, pp. 1–12, Dec. 2008.

[17] O. Benichou and F. Voituriez, "From first-passage times of random walks in confinement to geometry-controlled kinetics," *Physics Reports*, vol. 539, pp. 225–284, 2014.

[18] M. Jacob, S. Priebe, R. Dickhoff, T. Kleine-Ostmann, T. Schrader, and T. Kurner, "Diffraction in mm and sub-mm wave indoor propagation channels," *IEEE Transactions on Microwave Theory and Techniques*, vol. 60, pp. 833–844, Mar. 2012.

[19] I. Llatser, A. Cabellos-Aparicio, and M. Pierobon, "Detection techniques for diffusion-based molecular communication," *IEEE Journal on Selected Areas in Communications (JSAC)*, vol. 31, pp. 726–734, 2013.

[20] B. Oksendal, *Stochastic Differential Equations: An Introduction with Applications*. Springer, 2010.

[21] S. M. Ross, *Stochastic Processes*. John Wiley, 1996.

[22] M. Leeson and M. Higgins, "Forward error correction for molecular communications," in *Nano Communication Networks*, vol. 3, 2012.

[23] A. Noel, K. Cheung, and R. Schober, "Diffusive Molecular Communication with Disruptive Flows," in *IEEE International Conference on Communications (ICC)*, Jun. 2014, pp. 3600–3606.

[24] G. Wei, P. Bogdan, and R. Marculescu, "Efficient Modeling and Simulation of Bacteria-Based Nanonetworks with BNSim," *IEEE Journal on Selected Areas in Communications (JSAC)*, vol. 31, Dec. 2013.

[25] C. A. Balanis, *Advanced Engineering Electromagnetics*. Wiley, 1989.

[26] T. Rappaport, *Wireless Communications*. New Jersey, USA: Prentice-Hall, 2002.

[27] E. Jordan and K. Balmain, *Electromagnetic Waves and Radiating Systems*. Prentice Hall, 1968.

[28] N. Farsad, A. Eckford, S. Hiyama, and Y. Moritani, "On-chip molecular communication: Analysis and design," *IEEE Transactions on NanoBioscience*, vol. 11, no. 3, pp. 304–314, Feb. 2012.

[29] C. Mias and A. Freni, "Generalized wait-hill formulation analysis of lumped-element periodically-loaded orthogonal wire grid generic frequency selective surfaces," *Progress in Electromagnetics Research (PIER)*, vol. 143, pp. 47–66.

[30] A. Aragon-Zavala, B. Belloul, V. Nikolopoulos, and S. Saunders, "Accuracy evaluation analysis for indoor measurement-based radio-wave-propagation predictions," *IEE Proceedings Microwaves, Antennas and Propagation*, vol. 153, no. 1, pp. 67–74, Feb. 2006.